QUADRUPOLE ALIGNMENT AND TRAJECTORY CORRECTION FOR FUTURE LINEAR COLLIDERS: SLC TESTS OF A DISPERSION-FREE STEERING ALGORITHM[1]

R. Assmann, T. Chen, F.J. Decker, M. Minty,
T. Raubenheimer, R. Siemann
Stanford Linear Accelerator Center, Stanford, California 94309, USA

1 Introduction

The feasibility of future linear colliders depends on achieving very tight alignment and steering tolerances[2]. All proposals (NLC, JLC, CLIC, TESLA and S-BAND) currently require a total emittance growth in the main linac of less than 30-100% [1]. This should be compared with a 100% emittance growth in the much smaller SLC linac [2]. Major advances in alignment and beam steering techniques beyond those used in the SLC are necessary for the next generation of linear colliders. In this paper, we present an experimental study of quadrupole alignment with a dispersion-free steering algorithm. A closely related method (wakefield-free steering) takes into account wakefield effects [3]. However, this method can not be studied at the SLC.

The requirements for future linear colliders lead to new and unconventional ideas about alignment and beam steering. For example, no dipole correctors are foreseen for the standard trajectory correction in the NLC [4]; beam steering will be done by moving the quadrupole positions with magnet movers. This illustrates the close symbiosis between alignment, beam steering and beam dynamics that will emerge. It is no longer possible to consider the accelerator alignment as static with only a few surveys and realignments per year. The alignment in future linear colliders will be a dynamic process in which the whole linac, with thousands of beam-line elements, is aligned in a few hours or minutes, while the required accuracy of about 5 μm for the NLC quadrupole alignment [4] is a factor of 20 higher than in existing accelerators.

The major task in alignment and steering is the accurate determination of the optimum beam-line position. Ideally one would like all elements to be aligned along a straight line. However, this is not practical. Instead a “smooth curve” is acceptable as long as its wavelength is much longer than the betatron wavelength of the accelerated beam.

Conventional alignment methods are limited in accuracy by errors in the survey and the fiducials. Beam-based alignment methods ideally only depend upon the BPM resolution and generally provide much better precision. Many of those techniques are described in other contributions to this workshop. In this paper we describe our experiences with a dispersion-free steering algorithm for linacs. This algorithm was first suggested by Raubenheimer and Ruth in 1990 [5]. It h as been studied in simulations for NLC [5],

[1]Work supported by the Department of Energy, contract DE-AC03-76SF00515.

[2]Alignment and steering tolerances can be significantly loosened by the use of superconducting cavities as suggested for TESLA. Here we do not consider this approach.

TESLA [6], the S-BAND proposal [7] and CLIC [8]. The dispersion-free steering technique can be applied to the whole linac at once and returns the alignment (or trajectory) that minimizes the dispersive emittance growth of the beam. Thus it allows an extremely fast alignment of the beam-line.

As we will show dispersion-free steering is only sensitive to quadrupole misalignments. Wakefield-free steering [3] as mentioned before is a closely related technique that minimizes the emittance growth caused by both dispersion and wakefields. Due to hardware limitations (i.e. insufficient relative range of power supplies) we could not study this method experimentally in the SLC. However, its systematics are very similar to those of dispersion-free steering.

The studies of dispersion-free steering which are presented made extensive use of the unique potential of the SLC as the only operating linear collider. We used it to study the performance and problems of advanced beam-based optimization tools in a real beam-line environment and on a large scale. We should mention that the SLC has utilized beam-based alignment for years [9], using the difference of electron and positron trajectories. This method, however, cannot be used in future linear colliders. The goal of our work is to demonstrate the performance of advanced beam-based alignment techniques in linear colliders and to anticipate possible reality-related problems. Those can then be solved in the design state for the next generation of linear colliders.

2 Principle

The dispersion D(s) in any beam line is given by

$$D(s) = D_0 \cdot C(s) + D_0' \cdot S(s) + S(s) \cdot \int_{s_0}^{s} \frac{1}{\rho(t)} C(t)dt - C(s) \cdot \int_{s_0}^{s} \frac{1}{\rho(t)} S(t)dt \,, \qquad (1)$$

where *C(s)* and *S(s)* are the cosine-like and sine-like trajectories along the path length *s*, D_0 and D_0' are the initial dispersion and its derivative and ρ is the bending radius of the trajectory due to any transverse dipole fields. In a linac nominally there are no bending fields[3] so that all dispersion arises from quadrupole kicks $\Delta x \cdot K$ and corrector kicks θ. Here we neglect wakefield induced dispersion and RF-deflections. With a magnetic field gradient G_q and a beam energy of E we obtain the quadrupole strength K:

$$K[\mathrm{m}^{-2}] = \frac{0.03 \cdot G_q\,[\mathrm{kG/m}]}{E\,[\mathrm{GeV}]} \,. \qquad (2)$$

We get a similar formula for the corrector kick θ:

$$\theta\,[\mathrm{rad}] = \frac{0.03 \cdot B_c\,[\mathrm{kG}] \cdot L_c\,[\mathrm{m}]}{E\,[\mathrm{GeV}]} \,. \qquad (3)$$

In terms of dispersion a change in beam energy E is equivalent to a change in G_q or B_c. The dispersion can therefore be measured by scaling all quadrupole and corrector

[3] Some proposals anticipate “soft bends” in diagnostics stations along the linac.

strengths. This is a very useful approach because magnet strengths can be manipulated with much less systematic side effects than the overall beam energy (i.e. the beam energy profile E(s) is not measured in the SLC).

The principle of dispersion-free steering is illustrated in Fig. 1 for a simplified case. We assume that the BPM's are perfectly aligned to the centers of the quadrupoles and that there is only one misaligned quadrupole. The standard steering algorithm in the SLC minimizes the BPM readings and ideally will bump the beam through the center of the misaligned quadrupole (a). The resulting trajectory bump produces dispersion and dispersive emittance growth. The scaling of quadrupole and corrector strengths scales the bump in amplitude whilst the physical quadrupole position of course stays the same. As a result the beam experiences an additional deflection from the misaligned quadrupole which produces a downstream trajectory oscillation (b). From the oscillation we can calculate the quadrupole misalignment. This might be corrected by either realigning the quadrupole or by steering the beam off-center through the quadrupole and compensating the error locally using a corrector (c). Both possibilities are equivalent. In either case another scaling of quadrupoles and correctors would produce no change in trajectory. So the solution is dispersion-free. The power of the dispersion-free steering algorithm comes from its potential to analyze the superposition of many errors at once.

3 Setup and implementation

In the main linac of the SLC, wakefield effects are much stronger than those anticipated for the next generation of linear colliders. The presence of electrons and positrons in the same beam line introduces additional systematic problems which are not relevant, for future linear colliders. Dispersion-free steering was therefore tested with a special SLC setup:

1. A single bunch of electrons with about 1 x 10^{10} particles per bunch. The strength of wakefields was much reduced.

2. Beam feedback loops were switched off.

In order to measure dispersion the quadrupole and corrector strengths need to be scaled. Hysteresis effects were minimized by cycling the magnetic fields. With the lattice scale factor $\kappa = \Delta K / K$ the following hysteresis cycle was used:

$$\kappa = 1.00 \longrightarrow 0.90 \longrightarrow 0.80 \longrightarrow 0.70 \longrightarrow 1.05 \longrightarrow 1.00 \,. \qquad (4)$$

This cycle was executed as a first step and followed throughout the experiment to eliminate hysteresis. After the first initialization cycle so called measurement cycles were performed. The beam trajectory was measured with an average of 20 pulses for every scaling. The first four scalings were used for the dispersion-free steering data analysis which was performed for both planes simultaneously.

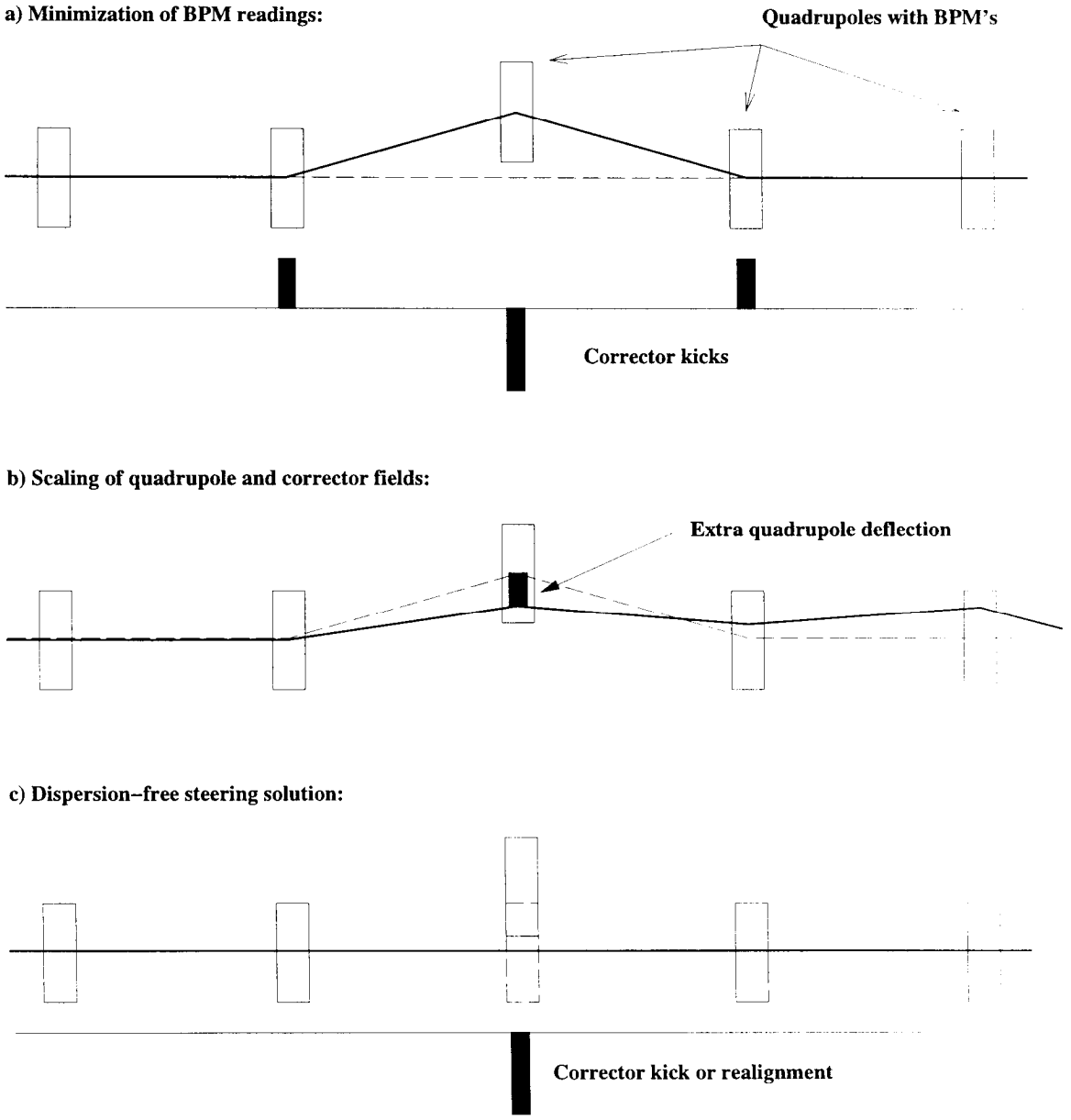

Figure 1: Illustration of the principle of dispersion-free steering. We assume one misaligned quadrupole and perfect BPM's that are fixed to the quadrupole centers. Each quadrupole has a corrector nearby. Minimizing the BPM readings with dipole corrector kicks leads to situation (a) where the beam is bumped through the center of the misaligned quadrupole. Scaling quadrupole and corrector strengths by the same amount (b) has no effect for the first quadrupole with perfect alignment. However, the "bump" is scaled and we see an extra deflection from the misaligned quadrupole. The induced downstream trajectory oscillation is a unique signature of the error. After realignment or correction (c) the quadrupole misalignment kick is eliminated or compensated by a corrector kick of the same magnitude but opposite sign. For dispersion-free steering we consider a superposition of many such errors.

Since the superposition of many errors generates the dispersion, a model for how a deflection at any location changes the trajectory at all downstream locations is required. Neglecting wakefield effects, the absolute reading x^j at a BPM *j* due to all upstream kicks θ_i is

$$x^j = \sum_{i=1}^{j-1} R_{12}^{i\to j}\,\theta_i\,, \tag{5}$$

where the transport matrix elements $R_{12}^{i\to j}$ from the kick *i* to the BPM *j* are given by

$$R_{12}^{i\to j} = \sqrt{\frac{E^i}{E^j}}\cdot\sqrt{\beta_x^i\cdot\beta_x^j}\cdot\sin\left[\psi_x^i-\psi_x^j\right]\,. \tag{6}$$

Here the $E^{i,j}$ are the beam energies, the $\beta_x^{i,j}$ are the beta functions and the $\psi_x^{i,j}$ are the betatron phase advances.

Now we calculate how the dispersive kicks change the difference trajectory Δx^j when the lattice is scaled. For the scaled lattice we need to recalculate the Twiss parameters (primed quantities). Then we have for Δx^j

$$\Delta x^j = x^j - x'^j = \sum_{i=1}^{j-1} R_{12,\kappa}^{i\to j}\,\theta_i\,, \tag{7}$$

where the $R_{12,\kappa}^{i\to j}$ are the transport matrix elements for the scaled lattice. We may neglect effects from non-linear dispersion since we use four different lattice scalings for our analysis. Then the dispersion-free solution must be local. Dispersion bumps are not easily possible and linear and non-linear dispersion are minimized simultaneously. For a. given lattice scaling κ the $R_{12,\kappa}^{i\to j}$ are

$$R_{12,\kappa}^{i\to j} = R_{12}^{i\to j} - \kappa\sqrt{\frac{E^i}{E^j}}\cdot\sqrt{\beta'^i_x\cdot\beta'^j_x}\cdot\sin\left[\psi'^i_x-\psi'^j_x\right]\,. \tag{8}$$

The Twiss parameters are calculated with the longitudinal magnet positions, the magnetic field values of the quadrupoles and the beam energy at each magnet.

The above model predicts the effect of dispersive kicks on the absolute trajectory x^j and the difference trajectories $\Delta x^j(\kappa)$. Alternatively, if we scale the lattice and measure x^j and $\Delta x^j(\kappa)$ we can use the model to calculate corrector settings that minimize both x^j and $\Delta x^j(\kappa)$. With four sets of measurements in each hysteresis cycle and *n* BPM's we

define the vector B of measurements as

$$B = \begin{bmatrix} x^1 \\ \Delta x^1(\kappa_1) \\ \Delta x^1(\kappa_2) \\ \Delta x^1(\kappa_3) \\ x^2 \\ \Delta x^2(\kappa_1) \\ \Delta x^2(\kappa_2) \\ \Delta x^2(\kappa_3) \\ \vdots \\ x^n \\ \Delta x^n(\kappa_1) \\ \Delta x^n(\kappa_2) \\ \Delta x^n(\kappa_3) \end{bmatrix}, \quad W = \begin{bmatrix} W^1 \\ W^1_\Delta(\kappa_1) \\ W^1_\Delta(\kappa_2) \\ W^1_\Delta(\kappa_3) \\ W^2 \\ W^2_\Delta(\kappa_1) \\ W^2_\Delta(\kappa_2) \\ W^2_\Delta(\kappa_3) \\ \vdots \\ W^n \\ W^n_\Delta(\kappa_1) \\ W^n_\Delta(\kappa_2) \\ W^n_\Delta(\kappa_3) \end{bmatrix}, \tag{9}$$

with W as the vector of weights. The κ_i correspond to different lattice scale factors κ. For each of the n BPM's we have four measured quantities. The weights are defined through inverse measurement errors. Let's first consider the absolute trajectory measurement x^j. Its measurement error has a statistical contribution $\sigma(x^j)$ from averaging 20 shots and a systematic contribution σ_{bpm} from the absolute BPM misalignment. The statistical error $\sigma(x^j)$ arises mainly from the BPM resolution and is usually well below 10 μm for the SLC. Because the individual BPM misalignments are unknown we assume their measured RMS Value for σ_{bpm}. The weight on x^j is then

$$W^j = \frac{1}{\sigma^2(x^j) + \sigma^2_{\text{bpm}}} . \tag{10}$$

Ideally the error on the measured trajectory difference Δx^j should only have the statistical contributions of the two measurements. However, a dispersion measurement in the SLC typically takes about 20 minutes and the error on Δx^j becomes dominated by the overall stability. From the observed trajectory drift and jitter we determined an additional systematic error σ_{sys} of 20 μm. The weights on Δx^j are then defined by

$$W^j_\Delta(\kappa_j) = \frac{1}{\sigma^2(x^j) + \sigma^2(x^j, \kappa_i) + \sigma^2_{\text{sys}}} . \tag{11}$$

Equations 10 and 11 define the x^2. By averaging 20 shots for each measurement the statistical errors are small and the x^2 is dominated by the two terms σ_{bpm} and σ_{sys}. We can write approximately

$$\chi^2 \approx \sum_j \left[\frac{x^{j2}}{\sigma^2_{\text{bpm}}} + \sum_{\kappa_i} \frac{\Delta x^{j2}(\kappa_i)}{\sigma^2_{\text{sys}}} \right] . \tag{12}$$

For the SLC σ_{bpm} is about 100 μm while the effective trajectory stability σ_{sys} during a hysteresis cycle is about 20 μm. The weight on a single "dispersion" measurement is about 25 times higher than that on the absolute trajectory. Therefore minimizing the dispersion makes optimum use of the BPM's and is much more efficient than solely minimizing the absolute trajectory. This is illustrated in Fig. 2 for the simplified x^2 of eq. 12. One can recognize the two extreme cases of only dispersion or only trajectory correction and the optimum combination of both.

We next define a correlation matrix

$$A = \begin{bmatrix} R_{12}^{1\to1} & 0 & \dots & 0 \\ R_{12,\kappa_1}^{1\to1} & 0 & \dots & 0 \\ R_{12,\kappa_2}^{1\to1} & 0 & \dots & 0 \\ R_{12,\kappa_3}^{1\to1} & 0 & \dots & 0 \\ R_{12}^{1\to2} & R_{12}^{2\to2} & \dots & 0 \\ R_{12,\kappa_1}^{1\to2} & R_{12,\kappa_1}^{2\to2} & \dots & 0 \\ R_{12,\kappa_2}^{1\to2} & R_{12,\kappa_2}^{2\to2} & \dots & 0 \\ R_{12,\kappa_3}^{1\to2} & R_{12,\kappa_3}^{2\to2} & \dots & 0 \\ \vdots & \vdots & \vdots & \vdots \\ R_{12}^{1\to n} & R_{12}^{2\to n} & \dots & R_{12}^{n\to n} \\ R_{12,\kappa_1}^{1\to n} & R_{12,\kappa_1}^{2\to n} & \dots & R_{12,\kappa_1}^{n\to n} \\ R_{12,\kappa_2}^{1\to n} & R_{12,\kappa_2}^{2\to n} & \dots & R_{12,\kappa_2}^{n\to n} \\ R_{12,\kappa_3}^{1\to n} & R_{12,\kappa_3}^{2\to n} & \dots & R_{12,\kappa_3}^{n\to n} \end{bmatrix} \tag{13}$$

and solve for the vector X of corrector settings:

$$\min_x ||W(B + AX)||_2 . \tag{14}$$

The solution X gives a set of corrector strengths that minimizes the trajectory and dispersion measurements simultaneously. Instead of solving for corrector kicks we could have solved for quadrupole positions that minimize the absolute trajectory and the dispersion.

4 SLC experiments

The dispersion-free steering algorithm was tested in early 1995 at the SLC. An example of trajectory and dispersion measurements after standard SLC steering is shown in Fig. 3. As explained earlier, four measurements are used to find a set of corrector settings that simultaneously minimizes both the absolute trajectory and the dispersion. In Fig. 4 the trajectory and dispersion measurements are shown for the same experiment but after three iterations of dispersion-free steering. The dispersion in this experiment was reduced by factors between 2 and 5. Because the SLC model does not describe the reality accurately it helped to do several iterations of dispersion-free steering. However, most of the dispersion reduction was achieved with the first round of dispersion-free steering.

The improvement in dispersion was confirmed by switching off a number of klystrons in the SLC. Thus the real beam energy is changed and the dispersion is independently measured. We found the same reduction in dispersion as from scaling the lattice.

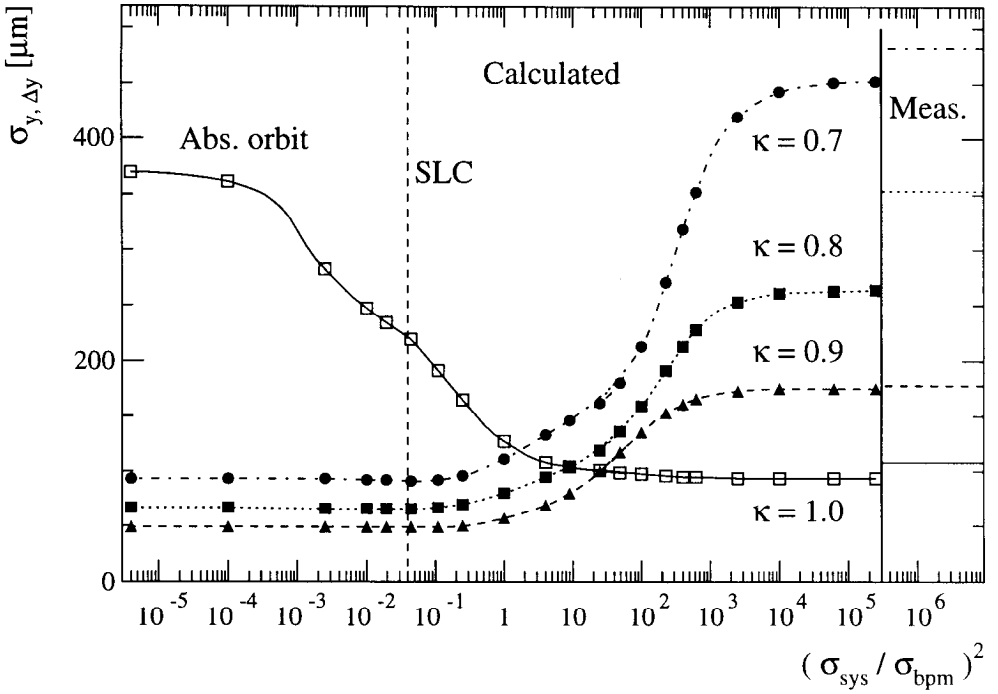

Figure 2: Dispersion and trajectory correction in SLC are shown for different relative weightings. The solid curve is the RMS of the absolute trajectory. The other curves show the RMS values of the difference trajectory for 3 lattice scalings. The ratio of σ_{sys} and σ_{bpm} is varied such that on the left hand side we have only dispersion correction and on the right hand side we have only trajectory correction. For the SLC values of σ_{sys} and σ_{bpm} we have some optimum combination of both. This data is calculated from measured data. On the right hand side the measured RMS values for pure trajectory correction are indicated.

The performance of dispersion-free steering during another experiment is shown in Figs. 5 and 6. For each lattice scaling we define the RMS deviation from zero as the relevant observable of trajectory or dispersion. Figures 5 and 6 show the measurements before and after dispersion-free steering (DFS) and both the calculated and the expected performances. Once the solution of the least-squares problem is found it can be used within the model to predict the absolute trajectory and dispersion measurements after correction. This we call the calculated performance. From the dominant terms σ_{bpm} and σ_{sys} in the x^2 we obtain the finally expected performance as σ_{bpm} for the absolute trajectory and σ_{sys} for the dispersion. We expect that the calculated and expected performances agree and that the measured performance agrees within small errors both with its calculated and expected value (assuming an accurate model). Although dispersion-free steering greatly reduced dispersion both the calculated and the measured performances are not as good as expected. We discuss this in the next section.

The RMS of the absolute trajectory in Figs. 5 and 6 is increased by dispersion-free

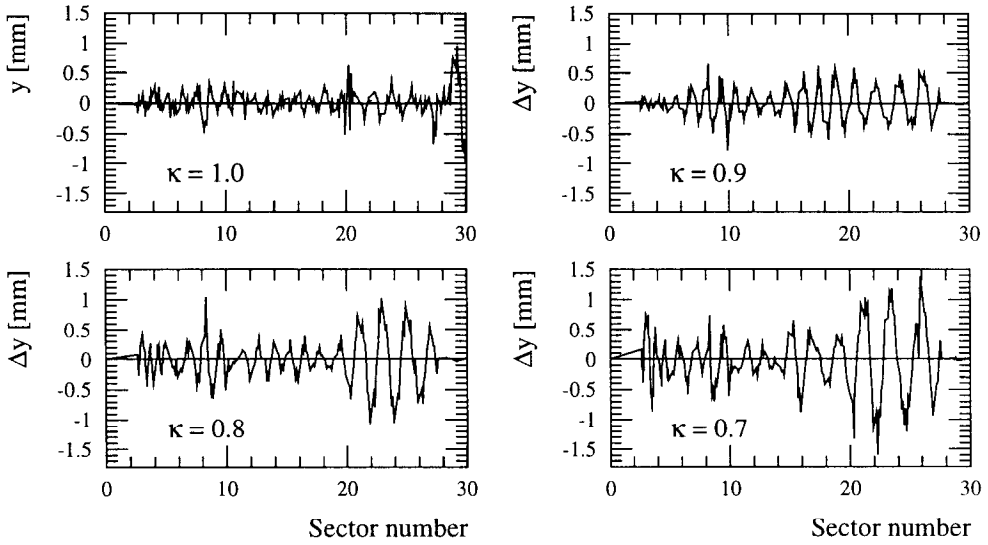

Figure 3: Absolute trajectory measurement (κ = 1.0) and difference measurements (κ = 0.9, 0.8, 0.7) for a cycle of lattice scaling in the SLC. The measurements were performed after standard trajectory steering in the SLC. The difference measurements are a measure of dispersion. Here, we scaled most of the SLC linac (sectors 2 to 26) by changing the magnet strengths.

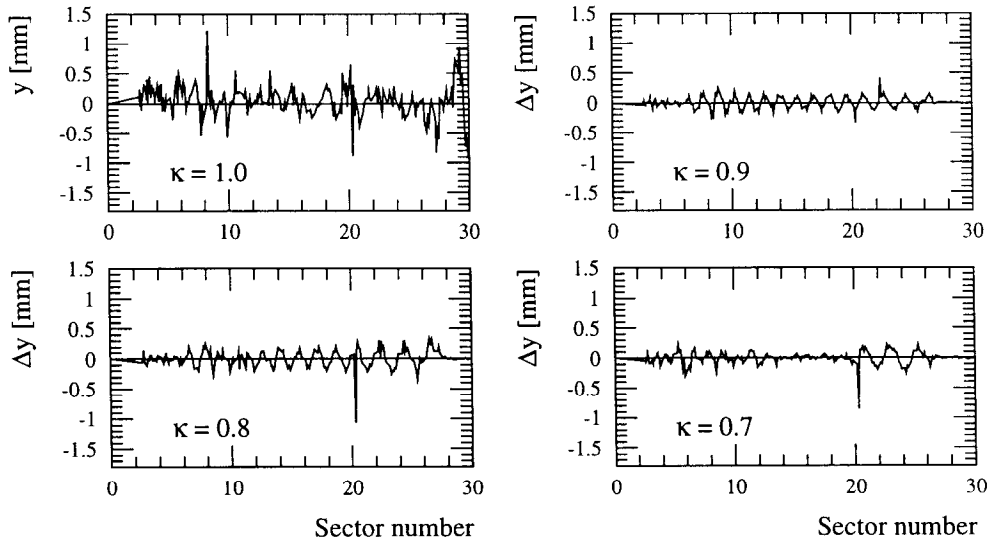

Figure 4: Absolute trajectory measurement (κ = 1.0) and difference measurements (κ = 0.9,0.8,0.7) for the same experiment as in Fig. 3 but after three iterations of dispersion-free steering; the dispersion signals are greatly reduced.

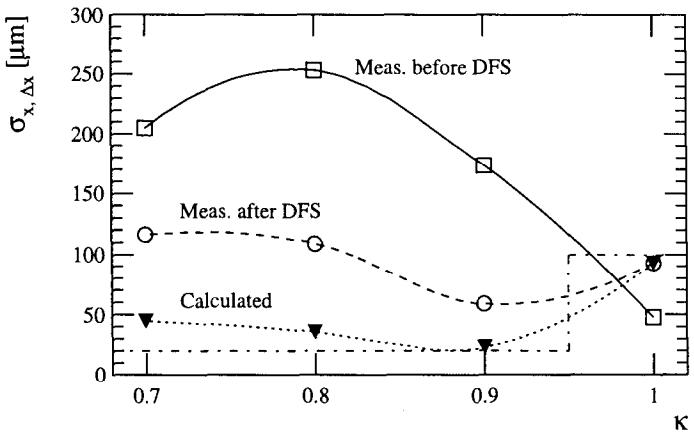

Figure 5: Summary from another dispersion-free steering experiment. For each lattice scaling, the RMS deviation in the horizontal plane is shown as the relevant observable. The four different curves show 1) the measurements after standard SLC trajectory correction and before dispersion-free steering (DFS), 2) the measurements after dispersion-free steering, 3) the calculated values from the least-squares solution and finally 4) the expected performance ($\sigma^x_{\rm bpm}$ and $\sigma^x_{\rm sys}$). The absolute trajectory measurement is shown at κ = 1. The lines connecting the points are to guide the eye and do not represent a functional dependence. Note that the dispersion in linear accelerators is not a closed solution as in storage rings and therefore is not proportional to κ.

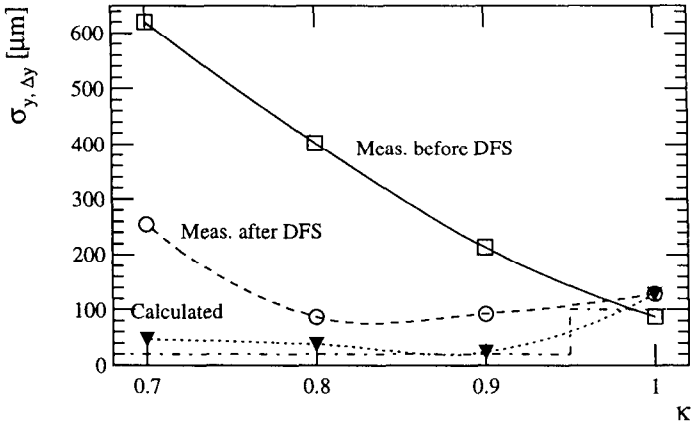

Figure 6: The same experiment and curves as in Fig. 5 are shown but for the vertical plane.

steering. This is expected since the alignment errors are no longer “hidden” by bumping the beam through the center of the BPM’s. They are locally compensated and therefore become “visible” to the BPM’s (compare Fig. 1).

5 Error discussion

In the previous section we have shown the performance of dispersion-free steering in the SLC at low current. Dispersion was greatly reduced but not down to the expected level. There are two problems:

1. Within our model, we could not calculate a dispersion-free solution that minimizes dispersion to its expected value of σ_{sys}.

2. The calculated performance of the dispersion-free solution was not reached during the experiments.

While dispersion was consistently reduced by factors of 2-5 we did not observe another factor of 4 due to those problems. We isolated two major explanations for the reduced efficiency of dispersion-free steering.

In the setup of the least-squares problem, we assume that misalignments and reading errors follow a Gaussian distribution. However, in reality non-Gaussian tails are observed. In this case, a few flyers can dominate the x^2 of the least-squares problem and significantly bias the solution. The x^2 per degree of freedom is larger than 1 and the dispersion solution does not reach its expected value. In Fig. 4, for example, the absolute trajectory y shows several large spikes that contribute almost 50% of the total x^2. Furthermore, one can observe corresponding spikes in the dispersion measurements Δy. Those strongly bias the solution of the least-squares problem. The spikes in the difference measurements are explained by non-linearities of the BPM’s. Especially BPM’s with large readings might not operate in their linear dynamic range and tend to behave non-linearly.

The problem of overpopulated tails can be avoided by cutting the tails such that they do not affect the data analysis any more. For this purpose we introduced a 2.5 sigma cut for y and 3.0 sigma cuts for the Δy. Those cuts eliminate some measurements from the least-squares fit. We still find a solution at the affected quadrupoles and BPM’s that however is unconstrained. Figure 7 shows the calculated dispersion-free solution with and without a cut on the tails. The analysis was done for the measurements that are shown in Fig. 4. In this case the cuts eliminated 5 of the 276 BPM’s from the data analysis. As a result the χ^2/DOF went down from 3.7 to 1.2 and the calculated dispersion is reduced to the expected value of $\sigma_{\mathrm{sys}} = 20\mu\mathrm{m}$. In future experiments we expect that this improved solution will help to reduce the measured dispersion beyond what was observed up to now.

Now we consider the second problem. If our model would accurately describe the reality we would expect complete agreement between the calculated and measured performances. However, the model we use does not include unknown linac imperfections.

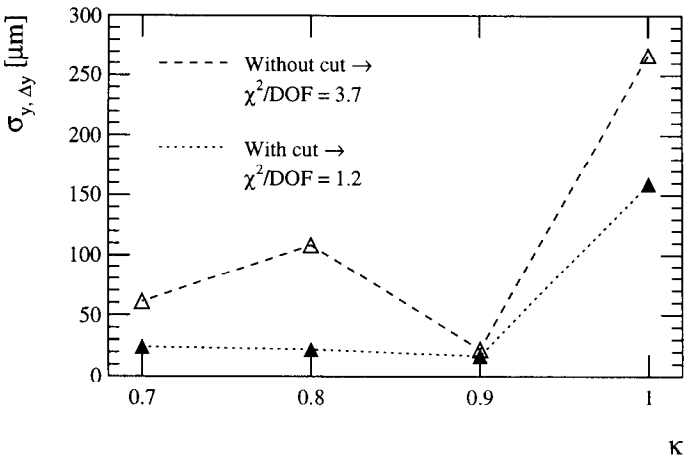

Figure 7: The calculated dispersion-free steering performance for the measurements in Fig. 4 is shown with and without a 2.5 sigma cut for *y* and 3.0 sigma cuts for the Δy. The cuts eliminate 5 of the 276 BPM's from the data analysis. As a result the χ^2/DOF is reduced from 3.7 to 1.2 and the calculated dispersion is reduced to its expected value of $\sigma_{\mathrm{sys}} = 20\mu\mathrm{m}$.

The effects of RF deflections and wakefield kicks due to misaligned RF structures are estimated to be roughly about 10 times smaller than those of quadrupole kicks. We do not expect to be limited from this at the moment. More serious are energy errors in the SLC that can cause large phase advance errors. In order to evaluate the validity of the model we used, we compared it with betatron oscillations in the SLC. A large disagreement, was found and soon explained by essentially one back-phased klystron. The first klystron in sector 3 of the SLC was actually deaccelerating the beam and induced a large relative energy error. This changed the phase advance along the linac by up to 180°. This error was not present during most of our experiments. However, later it was shown from the data of a diagnostic pulse [10] that all our experiments were affected by large unexpected phase advance errors in the SLC optics. They reduced the measured efficiency of the dispersion-free steering algorithm. The monitoring of the SLC optics will help in future experiments to avoid those errors.

6 Conclusion

The dispersion-free steering algorithm that has been suggested for future linear colliders was tested successfully in the SLC at low current. The dispersion was reduced by factors of $2\sim5$ as was shown with two independent methods (lattice scaling and energy changes).

Unexpected limitations in the performance of the dispersion-free steering algorithm were observed and explained by two main effects. First, large misalignments and non-linearities in the BPM readings dominated the x^2 and biassed the dispersion-free solution. This problem can be avoided by cutting the overpopulated non-Gaussian tails of the mea-

surements, thus allowing large misalignments at single quadrupoles without biassing the x^2. Second, errors in the SLC optics reduced the efficiency of the calculated dispersion-free solution. In linear accelerators, significant phase advance errors can easily be accumulated over its length. The monitoring of the optics with a diagnostic pulse could provide a more realistic optics model. Both limiting effects were previously not addressed in simulations. With the suggested improvements in the dispersion-free steering algorithm we expect to find a significantly improved performance of the method in future experiments at the SLC.

Finally, whether dispersion-free steering and the related algorithm of wakefield-free steering will be applied in the next linear collider will mainly depend on the time scales involved. Dispersion-free and wakefield-free steering allow a fast alignment of the linac in less than roughly 10 minutes. However, both methods are more sensitive to systematic errors than are local beam-based alignment methods that measure the relative alignment of each quadrupole versus BPM separately [11, 12]. Those local methods in turn are significantly slower. The stability of quadrupole and BPM alignment will in the end decide what method can be used with the highest efficiency.

7 Acknowledgements

We thank our SLC colleagues for the opportunity to study dispersion-free steering at the SLC. Many helped with support and advice: Nan Phinney, Marc Ross, Chris Adolphsen, Patrick Krejcik, Mark Woodley, Bill Spence, David Whittum and the SLC operators.

References

[1] Proceedings of the LC95.

[2] J.T. Seeman, F.J. Decker and I. Hsu: “The Introduction of Trajectory Oscillations to Reduce Emittance Growth in the SLC Linac”. SLAC-PUB-5705.

[3] T.O. Raubenheimer: “A New Technique of Correcting Emittance Dilutions in Linear Colliders”. Nucl. Instr. and Meth. A306(1991)61.

[4] C. Adolphsen et al., “Emittance and Energy Control in the NLC Main Linac”. Proc. of the 16th IEEE Particle Accelerator Conference (PAC95), Dallas, Texas, May 1-5, 1995.

[5] T.O. Raubenheimer and R.D. Ruth: “A Dispersion-Free Trajectory Correction Technique for Linear Colliders”. Nucl. Instr. and Meth. A302(1991)191.

[6] A. Mosnier: “Beam Instabilities Related to Different Focusing Schemes in TESLA”. TESLA report 93-22.

[7] M. Drevlak and R. Wanzenberg: “Beam Dynamics in the SBLC”. Internal Report DESY M-95-05.

[8] C. Fischer: “Improved CLIC Performances Using the Beam Response for Correcting Alignment Errors”. CERN/SL 95-19 (BI).

[9] C.E. Adolphsen et al., “Beam-Based Alignment Technique for the SLC Linac”. SLAC-PUB-4902.

[10] F.J. Decker et al., “Diagnostics Beam Pulses for Monitoring the SLC Linac”. SLAC-PUB-95-6880.

[11] M. Böge: “Beam-Based Alignment and Polarization Optimization in the HERA Electron Ring”. These proceedings.

[12] F. Tecker et al., “Dynamic Beam-Based Calibration of Orbit Monitors at LEP”. These proceedings.